

The parasitic helminth product ES-62 suppresses pathogenesis in CIA by targeting of the IL-17-producing cellular network at multiple sites

Miguel A Pineda Ph D¹, Mairi A McGrath Ph D¹, Pauline C Smith B Sc¹, Lamyaa Al-Riyami Ph D², Justyna Rzepecka Ph D², J Alastair Gracie Ph D¹, William Harnett Ph D² and Margaret M Harnett Ph D^{1*}

¹Institute of Infection, Immunity and Inflammation, Glasgow Biomedical Research Centre, University of Glasgow, 120 University Place, Glasgow G12 8TA, United Kingdom and

²Strathclyde Institute of Pharmacy and Biomedical Sciences, 161 Cathedral Street, Glasgow G4 0RE, United Kingdom

***Corresponding author:** Margaret M Harnett, Institute of Infection, Immunity and Inflammation, Glasgow Biomedical Research Centre, University of Glasgow, 120 University Place, Glasgow G12 8TA, United Kingdom; **tel:** +44-141-330-8413; **fax:** +44-141-330-4297; **e-mail:** Margaret.Harnett@glasgow.ac.uk

Running Title: ES-62 suppresses IL-17 production in collagen-induced arthritis

Funding: Funding from Arthritis Research UK, the Oliver Bird/Nuffield Foundation and the Wellcome Trust supported these studies. The authors have no conflicting financial interests.

Abbreviations: CIA: collagen-induced arthritis; PC: phosphorylcholine; RA: rheumatoid arthritis

This article has been accepted for publication and undergone full peer review but has not been through the copyediting, typesetting, pagination and proofreading process which may lead to differences between this version and the Version of Record. Please cite this article as an 'Accepted Article', doi: 10.1002/art.34581

© 2012 American College of Rheumatology

Received: Dec 06, 2011; Revised: Apr 11, 2012; Accepted: Jun 07, 2012

ABSTRACT

Objectives: Among many survival strategies, parasitic worms secrete molecules to modulate host immune responses. One such product, ES-62, is protective in the collagen-induced arthritis (CIA) model of rheumatoid arthritis. As IL-17 has been reported to play a pathological role in the development of rheumatoid arthritis, we investigated whether targeting of IL-17 may explain the protection afforded by ES-62 in the CIA model.

Methods: DBA/1 mice progressively display arthritis following immunization with type-II collagen. The protective effects of ES-62 were assessed by determination of cytokine levels, flow cytometric analysis of relevant cellular populations and *in situ* analysis of joint inflammation.

Results: ES-62 was found to downregulate IL-17 responses in the CIA model. Firstly, it acts to inhibit priming and polarisation of IL-17 responses by targeting a complex IL-17-producing network, involving signalling between dendritic cells and $\gamma\delta$ or CD4⁺ T cells. In addition, ES-62 directly targets Th17 cells by downregulating MyD88 expression to suppress responses mediated by IL-1 and TLR ligands. Moreover, ES-62 modulates migration of $\gamma\delta$ T cells and this is reflected by direct suppression of CD44 upregulation and, as evidenced by *in situ* analysis, dramatically reduced levels of IL-17-producing cells, including lymphocytes, infiltrating the joint. Finally, there is strong suppression of IL-17 production by cells resident in the joint, such as osteoclasts within the bone areas.

Conclusion: Such unique multi-site manipulation of the initiation and effector phases of the IL-17 inflammatory network could be exploited in the development of novel therapeutics for rheumatoid arthritis.

Key words: collagen-induced arthritis, inflammation, ES-62, IL-17

INTRODUCTION

Rheumatoid arthritis (RA) is a chronic autoimmune inflammatory condition, which, despite recent advances in cytokine therapy, continues to increase in incidence in the Western World. However, in areas of the world endemic for helminth infections, rates of autoimmune diseases such as RA remain low leading to the hypothesis that certain helminth infections may protect against the development of autoimmunity [1]. In support of this theory, we have previously shown that ES-62, a phosphorylcholine (PC)-containing glycoprotein secreted by the filarial nematode *Acanthocheilonema viteae*, has broad immunomodulatory activities and can exert powerful anti-inflammatory action in the mouse collagen-induced arthritis (CIA) model of RA [2, 3].

Originally it was proposed that the ability of ES-62 to inhibit disease severity in the CIA model reflected suppression of TNF- α production and associated Th1-mediated inflammation [2, 3]. However, it has become increasingly clear that Th17, rather than Th1 cells, appear to be the pathogenic drivers of inflammation in many autoimmune conditions, including CIA and RA [4]. Consistent with this, neutralization of IL-17 protects mice from disease, whilst over-expression of IL-17 exacerbates pathology [5]. Moreover, Th17 cells may be vital in promoting the chronic destructive phase of arthritis, due to their ability to induce the expression of RANKL and activate osteoclasts, thereby leading to bone resorption [6] as well as stimulating matrix metalloproteinases resulting in cartilage breakdown [7, 8]. Indeed, studies from RA patients have shown that IL-17 levels are raised in serum and synovial fluid samples compared to those from osteoarthritis or healthy control subjects [9]. By contrast, it has been proposed that IFN γ may play a protective role as IFN γ R^{-/-} mice are more susceptible to the development of CIA [10], perhaps reflecting abrogation of counter-regulation of Th17 development by IFN γ -producing Th1 cells [11]. Moreover, IFN γ is a potent antagonist of

osteoclastogenesis in mice and humans [12, 13] and thus may also act to prevent joint erosion.

Therefore, given these new insights into CIA pathology, it was important to ascertain the effect, if any, that ES-62, a molecule being considered in the context of therapeutic intervention, has on pro-inflammatory IL-17 production, and thus to re-address its protective role, but in the perspective of IL-17-associated pathology.

Accepted Article

MATERIALS AND METHODS

CIA

Animals were bred (BALB/c and C57BL/6 background) and/or maintained in the Biological Services Units in accordance with the Home Office UK Licences PPL60/3580, PPL60/3119 and PIL60/12183 and the Ethics Review Board of the University of Glasgow. CIA was induced in male DBA/1 mice (8-10 weeks old; Harlan Olac; Bicester, UK) by intradermal immunization with bovine type II collagen (CII, MD Biosciences) in complete Freund's adjuvant (FCA) and mice were treated with purified endotoxin-free ES-62 (2 µg/dose) or PBS subcutaneously on days -2, 0 and 21 [2, 3] and cells were recovered from joints [14] as previously described.

Ex vivo analysis

Draining lymph node (DLN) cells (10^6 /ml) were incubated \pm 50 ng/ml PMA plus 500 ng/ml ionomycin for 1 h before addition of 10 µg/ml Brefeldin A (Sigma-Aldrich, UK) for 5 h at 37°C with 5 % CO₂. Phenotypic markers were labelled using anti-TLR4-APC (R&D Systems), biotinylated anti-CD44 (BioLegend; detected by streptavidin-PE, BD Pharmingen), anti-CD4-PERCP or biotinylated anti-CD4 (detected by Alexa Fluor-450 streptavidin, BD Pharmingen), or anti- $\gamma\delta$ -FITC (BioLegend) antibodies before the cells were fixed and permeabilised using BioLegend protocols. Cells were then labelled using anti-IL-17A-APC or anti-IL-17A-PerCP-Cy5.5 (BioLegend), anti-ROR γ t (eBioscience; detected by anti-Rat IgG-APC) and anti-MyD88 (Abcam; detected by anti-Rabbit IgG-PE) antibodies for 30 min prior to flow cytometry, gated according to appropriate isotype controls.

Cytokine analysis

ELISAs for IL-17A, IL-10 (BioLegend), TNF- α , IL-6, IL-23 and IL-27 (eBioscience) were performed according to manufacturer's instructions. Alternatively, IL-17A was detected by cytometric bead assay (FlowCytomix).

In vitro cell culture

Bone marrow-derived dendritic cells (bmDCs) from male DBA/1, C57BL/6 or BALB/c mice (6-8 weeks old) were derived by *in vitro* culture in complete RPMI 1640 medium (containing 2 mM glutamine, 50 U/ml penicillin, 50 μ g/ml streptomycin and 10% FCS) supplemented with 10% conditioned medium from the GM-CSF-transfected X63 myeloma cell line and 50 μ M 2-ME at 37°C and in 5% CO₂ for 6d. Naïve CD4⁺CD62L⁺ T cells and $\gamma\delta$ T cells were isolated using Miltenyi magnetic bead technology. For bmDC-T cells co-cultures, bmDCs were incubated with ES-62 (2 μ g/mL), matured with LPS (*Salmonella minnesota*; Sigma) and then pulsed with ovalbumin (OVA) peptide (0-300 nM) before incubation with naïve T cells derived from OVA-specific DO.11.10/BALB/c or OT-II/C57BL/6 mice for 4d. For *in vitro* polarisation of Th17 cells, naïve LN T cells from BALB/c mice were incubated in plates pre-coated with anti-CD3 (4 μ g/mL) with anti-CD28 (1.5 μ g/mL), anti-IFN- γ (5 μ g/mL) and anti-IL-4 (5 μ g/mL) antibodies and rIL-6 (20 ng/mL), rTGF- β (4 ng/mL), and rIL-1 (10 ng/mL) \pm ES-62 (0-1 μ g/mL) for 4d. $\gamma\delta$ T cells from BALB/c mice were activated with rIL-1 + rIL-23 (both at 10 ng/mL) overnight \pm ES-62 (2 μ g/mL) before being incubated with bmDCs at different $\gamma\delta$:DC ratios (1:2, 1:5 and 1:20) and culture supernatants collected after 24 h.

Immunofluorescence

Tissue sections (7 μm) were deparaffinized in xylene, dehydrated in ethanol and antigen retrieved by incubation at 60°C for 2 h in 10 mM Tris-1 mM EDTA-0.05% Tween 20 buffer, pH 9.0. Samples were stained with a goat anti-mouse IL-17 antibody (R&D Systems; or goat IgG isotype control) and DAPI as counterstain, at 4°C for 12 h followed by a biotinylated rabbit anti-goat IgG antibody and streptavidin-Alexa Fluor 647. Images were obtained using a LSM510 meta confocal laser coupled to an Axiovert 200 (Zeiss) microscope and analyzed with the software Zeiss LSM Image Browser.

Laser Scanner Cytometry (LSC)

DLNs were fixed in 10% formalin at 4°C for 24 h, transferred to 30% sucrose in PBS for 48 h before being frozen in liquid nitrogen in OCT (Bayer) and stored at -70°C. Sections (7 μm) were stained with anti-B220-FITC and anti- $\gamma\delta$ TCR-PE (or isotype controls; BD Pharmingen) and mounted in Vectashield (Vector Laboratories). Quantitation of fluorescence was by LSC (CompuCyte) to generate tissue maps of the DLNs using WinCyte software version 3.6 (CompuCyte). Briefly, setting of a positive staining B220⁺ B cell gate generated a tissue map of the localisation of B220⁺ B cells that allowed generation of the indicated gates designating the paracortical (T cell area) and follicular (B220⁺ B cell area) regions that were subsequently copied onto the $\gamma\delta$ TCR⁺ T cell tissue map. This allowed unbiased statistical quantitation of $\gamma\delta$ TCR⁺ T cells within follicular regions by the WinCyte software following merging of $\gamma\delta$ TCR⁺ T cell and B220⁺ B cell tissue maps [15].

qRT-PCR

qRT-PCR and reverse transcription of RNA were according to the manufacturer's instructions (Applied Biosystems). HPLC purified probes (VH Bio; Integrated DNA technologies) contained the reporter 5'-6-carboxy-fluorescein (FAM) and quencher 3'-6-carboxy-tetramethyl rhodamine (TAMRA) dyes and sequences were: ROR γ t: F- 5'CCGCTGAGAGGGCTTCAC3', R- 5'TGCAGGAGTAGGCCACATTACA3' and 5'-FAM-AAGGGCTTCTTCCGCCGCCAGCAG-TAMRA-3'. Applied Biosystems assay kits for IL-17A, MyD88 and GAPDH (Mm00439618_m; NM_010851.2 and 4352339E1) were used. Data were analyzed by RQ Manager software (Applied Biosystems), normalized to the reference reporter GAPDH.

Statistics

Parametric data were analysed by the unpaired two-tailed Student's t test or by 1-way ANOVA followed by the Newman-Keuls post-test. Normalised data were analysed by the Kruskal-Wallis test whilst the Mann-Whitney test was used for analysis of clinical CIA scores where * $p < 0.05$, ** $p < 0.01$ and *** $p < 0.001$.

RESULTS

ES-62 protection against CIA is associated with down-regulation of IL-17 responses

ES-62 exhibits anti-inflammatory action in terms of significant reduction of articular score and hind paw swelling in mice undergoing CIA (Figure 1A). Disease incidence was also delayed and reduced in such ES-62-treated mice (Figure 1A). Consistent with IL-17 playing a pathogenic role in CIA, we observed a strong positive correlation of IL-17 (IL-17A), but not IFN γ , levels in serum with disease scores in animals with CIA (Figure 1B and results not shown). Thus to assess whether protection by ES-62 is associated with suppression of IL-17-mediated pathology, the effect of administration of the helminth product on serum cytokine levels was analyzed. Significantly higher levels of IL-17, but not IFN γ , were detected in the serum of mice with CIA, compared to naïve animals, and exposure to ES-62 *in vivo* reduced these towards the levels observed in naïve mice (Figure 1B and results not shown).

In accordance with this, significant differences between the PBS-, but not ES-62-, treated, and naïve groups mice were found in terms of total numbers of DLN cells (results not shown) and significantly higher proportions of DLN cells from CIA-PBS animals produced IL-17 relative to the ES-62-treated CIA mice following *ex vivo* stimulation with PMA plus ionomycin (Figure 1C). Moreover, although the differences did not reach statistical significance, analysis of spontaneous IL-17 production by cells recovered from the site of inflammation also showed a reduction in the proportion of IL-17⁺ cells infiltrating the joint in the ES-62 treated animals (Figure 1C). Corroboration that ES-62 suppressed Th17 responses was provided by data showing that ROR γ t mRNA levels were significantly lower in DLN cells from the ES-62-treated compared to PBS-treated CIA mice (Figure 1D). Targeting of ROR γ t and IL-17-associated responses by ES-62 was specific, since expression of the Th1-

associated transcription factor, t-Bet was not affected by exposure to the parasite product (data not shown).

ES-62 suppresses the levels of IL-17-producing CD4 and $\gamma\delta$ T cells

CD4 and $\gamma\delta$ T cells were the two major IL-17 producing compartments (>90%) in the DLN of all treatment groups (Figure 2A). Although the mice with CIA (PBS) tended to have higher numbers of DLN CD4⁺ T cells than those from both the naïve and ES-62-treated groups (Figure 2B), there were no significant differences amongst any of these groups, either in terms of proportions or absolute numbers of CD4⁺ T cells spontaneously producing IL-17 (results not shown). By contrast, following *ex vivo* stimulation with PMA plus ionomycin, whilst there were no differences in the proportions of such IL-17⁺ T cells (Figure 2C), significantly higher numbers of CD4⁺ T cells from the mice with CIA expressed IL-17 relative to the naïve group and this was reduced by exposure to ES-62 (Figure 2D). Analysis of $\gamma\delta$ T cell responses showed that there were no significant differences amongst the groups in terms of the total numbers of such cells present in the DLN (Figure 2B). However, both higher proportions and absolute numbers of $\gamma\delta$ T cells from the mice with CIA, but not those exposed to ES-62 *in vivo*, spontaneously produced IL-17 when compared to those from the naïve group (Figure 2C&D). No differences were detected amongst the groups, however, following *ex vivo* stimulation with PMA plus ionomycin (results not shown). Interestingly, whilst unlikely to be related to its protective effects (lack of serum IFN γ -disease correlation as mentioned earlier and [10]) we found that ES-62 suppressed the % of CD4⁺, $\gamma\delta$ ⁺ and CD8⁺ T cells spontaneously producing IFN γ (results not shown), data consistent with our previous reports that ES-62 suppressed IFN γ recall responses in CIA [2, 3].

ES-62 can attenuate Th17 responses by both indirect and direct effects

ES-62 modulates DC-mediated priming and polarisation of Th cell responses in healthy mice [16-18]. Thus, we next investigated whether ES-62 modulated the capacity of DC to prime Th17 responses in CIA by pre-incubating bmDC first derived from naïve DBA/1 mice with ES-62 before “maturing” them with LPS *in vitro*. Although LPS-stimulated release of IL-10 was unaffected (results not shown), we observed that ES-62 significantly inhibited the LPS-induced secretion of the pro-inflammatory cytokine, TNF- α and two cytokines associated with polarisation and survival of Th17 cells, IL-6 and IL-23 (Figure 3A). Similarly, bmDC derived from DBA/1 mice undergoing CIA (mean articular score of 7.1 ± 0.68) produced reduced levels of TNF- α , IL-6 and IL-23 when treated with ES-62 prior to LPS maturation, *in vitro* (Figure 3B). Moreover, whilst IL-23 could not be detected, bmDC derived from DBA/1 mice undergoing CIA (mean articular score 5.4 ± 1.6) spontaneously produced significantly more IL-6, but not TNF- α or IL-10, than those derived from either naïve DBA/1 (articular score 0) mice or DBA/1 mice undergoing CIA that had been exposed to ES-62 (mean articular score 1.8 ± 0.5) *in vivo* (Figure 3C and results not shown). Collectively, these findings suggested that ES-62 could suppress the generation of Th17-polarising cytokines by DC in CIA, and consistent with this ES-62-treated DCs show a reduced ability to skew naïve OVA-specific T cells towards a Th17 phenotype (Figure 3D).

We next investigated whether ES-62 could also directly affect Th17 cells. Naïve T cells were primed using anti-CD3 plus anti-CD28 antibodies in the presence of the cytokines, IL-6, TGF β and IL-1 β and neutralizing antibodies specific for IFN γ and IL-4 to induce *in vitro* differentiation of Th17 cells. When co-incubated with the parasite product, we observed that ES-62 was able to directly down-regulate IL-17 production in a significant and dose-

dependent manner and this reduction in IL-17 release was reflected by reduced IL-17 mRNA levels (Figure 4A). We found expression of TLR4, which is required for ES-62 action [19], to be up-regulated during *in vitro* priming and differentiation of Th17 cells, in parallel with that of MyD88 and ROR γ t (Figure 4B). From a mechanistic point of view, whilst ES-62 did not appear to modulate either the surface or intracellular levels of TLR4 (data not shown), it did induce downregulation of the TLR signal transducer, MyD88 (Figure 4C) and this was also reflected at the mRNA level (Figure 4D).

DCs are necessary for ES-62-targeting of IL-17 production by $\gamma\delta$ T cells

To address whether ES-62 could likewise directly modulate IL-17 production by $\gamma\delta$ T cells, $\gamma\delta$ T cells from naïve mice were stimulated to produce IL-17 *in vitro* in a TCR-independent manner using rIL-1+rIL-23 [20]. Such “activated”, but not resting, $\gamma\delta$ T cells produced large amounts of IL-17. However, ES-62 did not modulate this response (Figure 5A) and perhaps consistent with this, we could not detect TLR4 expression and culture with LPS did not induce $\gamma\delta$ T cell activation (results not shown). Nevertheless, we found that ES-62 could inhibit $\gamma\delta$ T cell activation as indicated by its ability to prevent upregulation of the cell surface marker CD44 *in vitro* (Figure 5A) and *in vivo* (Figure 5B).

We therefore next investigated whether DCs were regulating production of IL-17 by $\gamma\delta$ T cells by co-culturing LPS-matured DCs with resting or IL-1/IL-23-stimulated $\gamma\delta$ cells that had been exposed or not to ES-62 and found that IL-17 production was reduced in such ES-62-treated DC- $\gamma\delta$ T cell co-cultures at all ratios tested (Figure 5C). Furthermore, IL-17 and ROR γ t mRNA levels were also reduced when the activated $\gamma\delta$ T cells had been exposed to ES-62 (Figure 5C). DC maturation is required for these conditioning effects on $\gamma\delta$ T cells as such immunomodulation did not occur with immature DCs. Also, whilst the results did not reach significance, the observed effects were associated with increased generation of IL-27, a

cytokine that antagonises IL-17 production [21, 22], in the co-cultures containing ES-62-treated $\gamma\delta$ T cells (results not shown).

ES-62-mediated modulation of $\gamma\delta$ T cell responses also appears to occur during CIA *in vivo*. Thus, such DLN $\gamma\delta$ T cells not only displayed reduced expression of CD44 when analysed *ex vivo* (Figure 5B) but also *in situ* analysis demonstrated that $\gamma\delta$ T cells in such ES-62-treated mice exhibited altered localisation within DLN, showing reduced distribution in the B cell follicles compared to those from PBS-treated CIA animals (Figure 5D).

ES-62 reduces the levels of IL-17 positive cells in the joints of CIA animals

Consistent with a pathogenic effector role for IL-17 in the joint, *in situ* analysis showed that whilst little or no IL-17 expression could be detected in the joints of naïve mice (Figure 6A), there was strong expression of this cytokine in the joints from PBS-treated CIA mice, (articular scores 7&8). By contrast, expression of IL-17 was dramatically reduced in the joints of ES-62-treated mice (articular scores 3&0). Furthermore, examination of the cells producing IL-17 indicated that this reflected cells both infiltrating the joint (Figure 6B&C), including large numbers of lymphocytes as indicated by size and morphology (Figure 6C), as well as those in the bone such as multinucleated osteoclasts (Figures 6B). IL-17 produced at both sites appeared to be reduced in mice treated with ES-62 (Figure 6A). These data suggest that as well as suppressing early IL-17-driven pro-inflammatory responses in the DLN associated with the initiation of pathogenesis, exposure to ES-62 *in vivo* is able to reduce effector IL-17 responses in the affected joints.

DISCUSSION

The recent proposal that IL-17 is a master regulator of CIA pathogenesis suggested that targeting of cellular producers of this cytokine might provide a mechanism for suppression of disease severity by ES-62 [2, 3]. Consistent with this, the highly elevated levels of IL-17 in the serum of mice with CIA, compared to naïve animals, were significantly reduced in the ES-62-treated CIA cohorts. Furthermore, ES-62 reduced the percentage of IL-17⁺ DLN cells, relative to their control CIA cohorts, such that these were not significantly different to those of naïve DBA/1 mice. Although, prophylactic treatment with ES-62 at d-2, -0 and -21 results in some 50-60 % suppression of articular score, it is likely that more frequent and/or higher doses of ES-62 would have further reduced IL-17 responses and resultant pathology.

Alternatively, since ES-62 typically reduces IL-17 responses towards the levels observed in naïve DBA/1 mice, the residual pathology observed in the presence of ES-62 could reflect IL-17-independent pathogenic effector mechanisms. However, it is certainly the case that CD4⁺ and $\gamma\delta$ T cell-driven pathogenesis in CIA relies on the ability of these cells to initiate IL-17 dependent responses [14, 23-25], albeit, it has recently been suggested that the induction of $\gamma\delta$ T cells may be as a result of CFA-associated inflammation [14, 23]. However, we found that the levels of IL-17⁺ $\gamma\delta$ T cells were not up-regulated in mice immunized with CFA alone (results not shown), indicating that IL-17 production by both CD4⁺ and $\gamma\delta$ T cells plays a role in the collagen response and importantly, ES-62 targets both of these major IL-17 producing compartments in our CIA model.

DCs are a major target of ES-62 action in modulating priming and polarisation of Th cell responses [16-18]. Thus, we hypothesised that the reduction in Th17 cells reflected suppression of Th17 cell priming by DCs. We subsequently found that *in vitro* conditioning of bmDC with ES-62 significantly inhibited LPS-driven production of TNF- α , IL-6 and IL-

23, the latter two cytokines implicated in the development and maintenance of the Th17-phenotype, and a reduction of OVA-specific priming of IL-17 production by naïve CD4⁺ Th cells. However we also observed that ES-62 could modulate Th17 responses, directly. Although naïve CD4⁺ T cells do not express TLR4, the receptor required for ES-62 to mediate its anti-inflammatory effects in APC [19, 26], we found upregulation of TLR4 and MyD88 in parallel with the signature transcription factor, ROR γ t during *in vitro* polarisation to the Th17 phenotype. ES-62-mediated suppression of the resultant IL-17 response therefore likely reflects not only that TLRs can be expressed by most T cell subsets, but also that TLR agonists (e.g. for TLR3, 5, 7 and 9) can modulate effector or regulatory T cell responses in the absence of APC (reviewed in [27]) and LPS/TLR4 signalling can both induce and enhance IL-23-stimulated IL-17 release from *in vitro* differentiated Th17 cells [28]. We find that ES-62 suppresses IL-17 release from Th17 cells differentiated *in vitro* in response to IL-1 but not in response to IL-23 (manuscript in preparation), a cytokine that has been shown to commit naïve T cells to a Th17 phenotype via STAT-3 activation independently of MyD88 recruitment [29]. Therefore, ES-62 subversion of signalling via TLR4 with consequent downregulation of MyD88, a key signal transducer of the TLR/IL-1R family [30], would provide a molecular rationale for the observed decrease in Th17 polarisation given that it has recently been reported [31, 32] that IRAK4 and IRAK1, the downstream effectors of IL-1R/MyD88 signalling are required for such polarisation.

By contrast, ES-62 did not directly down-regulate IL-17 production by $\gamma\delta$ T cells in response to activation with IL-1/IL-23 and consistent with this, we were unable to detect TLR4 expression by $\gamma\delta$ T cells, supporting the proposal that modulation of $\gamma\delta$ T cell responses by LPS requires cooperation with DCs [33]. It was surprising therefore that we found that ES-62 suppressed the upregulation of CD44 resulting from activation of $\gamma\delta$ T cells in response to IL-

1/IL-23. These data suggested that ES-62 might directly modulate $\gamma\delta$ T cell activation, but not cytokine production, through some undefined receptor like those involved in recognition of small phosphorylated molecules present in Mycobacteria that lead to DC activation by $\gamma\delta$ T cells [34, 35] in a TLR-independent manner [36-39]. In turn, mature DCs can stimulate $\gamma\delta$ T cells to promote sustained immune responses [37, 40] and perhaps of relevance to this study, DCs have been shown to modulate IL-17 production by $\gamma\delta$ T cells [41]. Thus as the active phosphorylcholine moiety of ES-62 [3] is structurally reminiscent of the phosphorylated mycobacterial molecules, this suggested that ES-62 was possibly targeting $\gamma\delta$ T cells via such receptors to modulate bi-directional interaction with DC, a hypothesis supported by ES-62 downregulating IL-17 and tending to upregulate IL-27, a cytokine that suppresses CIA [22, 42, 43], production in DC: $\gamma\delta$ co-cultures.

The targeting of CD44 expression by $\gamma\delta$ T cells observed *in vitro* and *in vivo* may be physiologically relevant to ES-62-mediated protection from CIA as such modulation would impact on lymphocyte migration during CIA [44], particularly to the joint [45]. Indeed, *in situ* LSC revealed that exposure to ES-62 *in vivo* modulates the localisation of $\gamma\delta$ T cells within the DLN of mice with CIA and this may in turn modulate bidirectional signalling between $\gamma\delta$ T cells and DC, to subvert initiation of the inflammatory phenotype driving autoimmunity. Moreover, and perhaps reflecting suppression of CD44-mediated migration of IL-17-producing lymphocytes to the site of inflammation, we have also shown that ES-62 can dramatically reduce the levels of IL-17⁺ infiltrating cells in the joints. This is likely to be of importance therapeutically as IL-17 produced during the initiator phase, induces the recruitment and accumulation of inflammatory cells, particularly neutrophils to the joints and the release of pro-inflammatory chemokines, cytokines and matrix metalloproteinases [7, 8, 46], that ultimately results in osteoclastogenesis and bone destruction *in situ* [47].

Interestingly, our data suggest that during the effector phase, infiltrating cells and bone cells could both be producing IL-17 *in situ*, as some of the IL-17⁺ cells in the bone appear multinucleated (Figure 6B), suggesting that they could be osteoclasts. Moreover, the infiltrating cells in the joints of mice with CIA contain large numbers of small IL-17⁺ mononuclear cells that appear to be lymphocytes, consistent with ES-62 blocking the migration of pathogenic effector Th17 and/or IL-17-producing $\gamma\delta$ T cells to the site of inflammation. Importantly, levels of all classes of IL-17 producing cells in the joint appear to be reduced in the ES-62-treated mice.

Collectively, these data suggest that ES-62 targets the IL-17 inflammatory axis at several regulatory points in order to optimize safe modulation of pathogenic IL-17 responses (Figure 6D). Thus, it both targets cells of the innate immune system (DCs and $\gamma\delta$ T cells) to inhibit initiation of pathogenic responses and also, by acting directly on Th17 cells, suppress ongoing adaptive responses. Mechanistically, given the increasing evidence for TLR signalling in the initiation (DC) and amplification of Th17 and $\gamma\delta$ T cell-mediated IL-17 responses and autoimmune inflammation [28, 31, 48], it is pertinent that ES-62 rewires TLR-2, -4 and -9 driven maturation of DC to an anti-inflammatory phenotype in a TLR4-dependent manner [19]. This is reflected here by the inhibition of LPS-induced TNF- α , IL-6 and IL-23 production as well as increased IL-27 release, resulting in suppression of differentiation and/or maintenance of the Th17 phenotype. ES-62 can also act directly on CD4⁺ T cells to suppress IL-1-dependent Th17 differentiation and this likely involves TLR4-mediated downregulation of MyD88, leading to un-coupling of IL-1R from IRAK1/4 signals that are essential for Th17 polarisation [31, 32]. As MyD88 is a key signal transducer for all TLR family members except for TLR3 (interestingly, signalling of which is not modulated by ES-62 [19]), the recent finding that Th17 responses and consequent autoimmune

pathogenesis are promoted by TLR2 signalling *in vivo* [28] suggests that ES-62 may downregulate MyD88 expression as a general mechanism of targeting aberrant Th17 responses and inflammatory disease. Interestingly, ES-62 also acts directly on $\gamma\delta$ T cells, possibly via phosphoantigen receptors (pAgR), not only to modulate the bidirectional DC- $\gamma\delta$ interactions required to drive subsequent adaptive Th17 responses, but also to downregulate CD44 expression and suppress migration of such pathogenic cells to the joints. Certainly, it dramatically suppresses pathogenic IL-17 production by effector cells within the joint.

Hence, the use of ES-62 to modulate this highly inflammatory mediator by targeting both DC maturation and effector T cell responses through subversion of TLR4 signalling, without compromising the host immune response to infection [26], constitutes a highly appealing therapeutic strategy for RA.

REFERENCES

1. Cooke, A., Zaccane, P., Raine, T., Phillips, J.M., Dunne, D.W. 2004. Infection and autoimmunity: are we winning the war, only to lose the peace? *Trends Parasitol*, 20: 316-21.
2. McInnes, I.B., Leung, B.P., Harnett, M., Gracie, J.A., Liew, F.Y., Harnett, W. 2003. A novel therapeutic approach targeting articular inflammation using the filarial nematode-derived phosphorylcholine-containing glycoprotein ES-62. *J Immunol*, 171: 2127-33.
3. Harnett, M.M., Kean, D.E., Boitelle, A., McGuinness, S., Thalhamer, T., Steiger, C.N., Egan, C., Al-Riyami, L., Alcocer, M.J., Houston, K.M. *et al.* 2008. The phosphorylcholine moiety of the filarial nematode immunomodulator ES-62 is responsible for its anti-inflammatory action in arthritis. *Ann Rheum Dis*, 67: 518-23.
4. Nakae, S., Nambu, A., Sudo, K., Iwakura, Y. 2003. Suppression of immune induction of collagen-induced arthritis in IL-17-deficient mice. *J Immunol*, 171: 6173-7.
5. Koenders, M.I., Lubberts, E., Oppers-Walgreen, B., van den Bersselaar, L., Helsen, M.M., Kolls, J.K., Joosten, L.A., van den Berg, W.B. 2005. Induction of cartilage damage by overexpression of T cell interleukin-17A in experimental arthritis in mice deficient in interleukin-1. *Arthritis Rheum*, 52: 975-83.
6. Sato, K., Suematsu, A., Okamoto, K., Yamaguchi, A., Morishita, Y., Kadono, Y., Tanaka, S., Kodama, T., Akira, S., Iwakura, Y. *et al.* 2006. Th17 functions as an osteoclastogenic helper T cell subset that links T cell activation and bone destruction. *J Exp Med*, 203: 2673-82.
7. Benderdour, M., Tardif, G., Pelletier, J.P., Di Battista, J.A., Reboul, P., Ranger, P., Martel-Pelletier, J. 2002. Interleukin 17 (IL-17) induces collagenase-3 production in

- human osteoarthritic chondrocytes via AP-1 dependent activation: differential activation of AP-1 members by IL-17 and IL-1beta. *J Rheumatol*, 29: 1262-72.
8. Koshy, P.J., Henderson, N., Logan, C., Life, P.F., Cawston, T.E., Rowan, A.D. 2002. Interleukin 17 induces cartilage collagen breakdown: novel synergistic effects in combination with proinflammatory cytokines. *Ann Rheum Dis*, 61: 704-13.
9. Shahrara, S., Huang, Q., Mandelin, A.M., 2nd, Pope, R.M. 2008. TH-17 cells in rheumatoid arthritis. *Arthritis Res Ther*, 10: R93.
10. Vermeire, K., Heremans, H., Vandeputte, M., Huang, S., Billiau, A., Matthys, P. 1997. Accelerated collagen-induced arthritis in IFN-gamma receptor-deficient mice. *J Immunol*, 158: 5507-13.
11. Chu, C.Q., Swart, D., Alcorn, D., Tocker, J., Elkon, K.B. 2007. Interferon-gamma regulates susceptibility to collagen-induced arthritis through suppression of interleukin-17. *Arthritis Rheum*, 56: 1145-51.
12. Takayanagi, H., Ogasawara, K., Hida, S., Chiba, T., Murata, S., Sato, K., Takaoka, A., Yokochi, T., Oda, H., Tanaka, K. *et al.* 2000. T-cell-mediated regulation of osteoclastogenesis by signalling cross-talk between RANKL and IFN-gamma. *Nature*, 408: 600-5.
13. Yago, T., Nanke, Y., Kawamoto, M., Furuya, T., Kobashigawa, T., Kamatani, N., Kotake, S. 2007. IL-23 induces human osteoclastogenesis via IL-17 in vitro, and anti-IL-23 antibody attenuates collagen-induced arthritis in rats. *Arthritis Res Ther*, 9: R96.
14. Roark, C.L., French, J.D., Taylor, M.A., Bendele, A.M., Born, W.K., O'Brien, R.L. 2007. Exacerbation of collagen-induced arthritis by oligoclonal, IL-17-producing gamma delta T cells. *J Immunol*, 179: 5576-83.

15. Marshall, F.A., Grierson, A.M., Garside, P., Harnett, W., Harnett, M.M. 2005. ES-62, an immunomodulator secreted by filarial nematodes, suppresses clonal expansion and modifies effector function of heterologous antigen-specific T cells in vivo. *J Immunol*, *175*: 5817-26.
16. Whelan, M., Harnett, M.M., Houston, K.M., Patel, V., Harnett, W., Rigley, K.P. 2000. A filarial nematode-secreted product signals dendritic cells to acquire a phenotype that drives development of Th2 cells. *J Immunol*, *164*: 6453-60.
17. Goodridge, H.S., Marshall, F.A., Wilson, E.H., Houston, K.M., Liew, F.Y., Harnett, M.M., Harnett, W. 2004. In vivo exposure of murine dendritic cell and macrophage bone marrow progenitors to the phosphorylcholine-containing filarial nematode glycoprotein ES-62 polarizes their differentiation to an anti-inflammatory phenotype. *Immunology*, *113*: 491-8.
18. Goodridge, H.S., McGuinness, S., Houston, K.M., Egan, C.A., Al-Riyami, L., Alcocer, M.J., Harnett, M.M., Harnett, W. 2007. Phosphorylcholine mimics the effects of ES-62 on macrophages and dendritic cells. *Parasite Immunol*, *29*: 127-37.
19. Goodridge, H.S., Marshall, F.A., Else, K.J., Houston, K.M., Egan, C., Al-Riyami, L., Liew, F.Y., Harnett, W., Harnett, M.M. 2005. Immunomodulation via novel use of TLR4 by the filarial nematode phosphorylcholine-containing secreted product, ES-62. *J Immunol*, *174*: 284-93.
20. Sutton, C.E., Lator, S.J., Sweeney, C.M., Brereton, C.F., Lavelle, E.C., Mills, K.H. 2009. Interleukin-1 and IL-23 induce innate IL-17 production from gammadelta T cells, amplifying Th17 responses and autoimmunity. *Immunity*, *31*: 331-41.
21. Feng, T., Qin, H., Wang, L., Benveniste, E.N., Elson, C.O., Cong, Y. 2011. Th17 cells induce colitis and promote Th1 cell responses through IL-17 induction of innate IL-12 and IL-23 production. *J Immunol*, *186*: 6313-8.

22. Murugaiyan, G., Mittal, A., Lopez-Diego, R., Maier, L.M., Anderson, D.E., Weiner, H.L. 2009. IL-27 is a key regulator of IL-10 and IL-17 production by human CD4+ T cells. *J Immunol*, 183: 2435-43.
23. Ito, Y., Usui, T., Kobayashi, S., Iguchi-Hashimoto, M., Ito, H., Yoshitomi, H., Nakamura, T., Shimizu, M., Kawabata, D., Yukawa, N. *et al.* 2009. Gamma/delta T cells are the predominant source of interleukin-17 in affected joints in collagen-induced arthritis, but not in rheumatoid arthritis. *Arthritis Rheum*, 60: 2294-303.
24. Harrington, L.E., Mangan, P.R., Weaver, C.T. 2006. Expanding the effector CD4 T-cell repertoire: the Th17 lineage. *Curr Opin Immunol*, 18: 349-56.
25. Langrish, C.L., Chen, Y., Blumenschein, W.M., Mattson, J., Basham, B., Sedgwick, J.D., McClanahan, T., Kastelein, R.A., Cua, D.J. 2005. IL-23 drives a pathogenic T cell population that induces autoimmune inflammation. *J Exp Med*, 201: 233-40.
26. Al-Riyami L., H.W. 2011. Immunomodulatory Properties of ES-62, a Phosphorylcholine - Containing Glycoprotein Secreted by *Acanthocheilonema viteae*. *Endocrine, Metabolic & Immune Disorders - Drug targets*, in press.
27. Kulkarni, R., Behboudi, S., Sharif, S. 2011. Insights into the role of Toll-like receptors in modulation of T cell responses. *Cell Tissue Res*, 343: 141-52.
28. Reynolds, J.M., Pappu, B.P., Peng, J., Martinez, G.J., Zhang, Y., Chung, Y., Ma, L., Yang, X.O., Nurieva, R.I., Tian, Q. *et al.* 2010. Toll-like receptor 2 signaling in CD4(+) T lymphocytes promotes T helper 17 responses and regulates the pathogenesis of autoimmune disease. *Immunity*, 32: 692-702.
29. Ivanov, II, Zhou, L., Littman, D.R. 2007. Transcriptional regulation of Th17 cell differentiation. *Semin Immunol*, 19: 409-17.
30. Kenny, E.F., O'Neill, L.A. 2008. Signalling adaptors used by Toll-like receptors: an update. *Cytokine*, 43: 342-9.

31. Gulen, M.F., Kang, Z., Bulek, K., Youzhong, W., Kim, T.W., Chen, Y., Altuntas, C.Z., Sass Bak-Jensen, K., McGeachy, M.J., Do, J.S. *et al.* 2010. The receptor SIGIRR suppresses Th17 cell proliferation via inhibition of the interleukin-1 receptor pathway and mTOR kinase activation. *Immunity*, 32: 54-66.
32. Staschke, K.A., Dong, S., Saha, J., Zhao, J., Brooks, N.A., Hepburn, D.L., Xia, J., Gulen, M.F., Kang, Z., Altuntas, C.Z. *et al.* 2009. IRAK4 kinase activity is required for Th17 differentiation and Th17-mediated disease. *J Immunol*, 183: 568-77.
33. Shibata, K., Yamada, H., Hara, H., Kishihara, K., Yoshikai, Y. 2007. Resident Vdelta1+ gammadelta T cells control early infiltration of neutrophils after Escherichia coli infection via IL-17 production. *J Immunol*, 178: 4466-72.
34. Conti, L., Casetti, R., Cardone, M., Varano, B., Martino, A., Belardelli, F., Poccia, F., Gessani, S. 2005. Reciprocal activating interaction between dendritic cells and pamidronate-stimulated gammadelta T cells: role of CD86 and inflammatory cytokines. *J Immunol*, 174: 252-60.
35. Tanaka, Y., Brenner, M.B., Bloom, B.R., Morita, C.T. 1996. Recognition of nonpeptide antigens by T cells. *J Mol Med (Berl)*, 74: 223-31.
36. Petermann, F., Rothhammer, V., Claussen, M.C., Haas, J.D., Blanco, L.R., Heink, S., Prinz, I., Hemmer, B., Kuchroo, V.K., Oukka, M. *et al.* 2010. gammadelta T cells enhance autoimmunity by restraining regulatory T cell responses via an interleukin-23-dependent mechanism. *Immunity*, 33: 351-63.
37. Collins, C., Shi, C., Russell, J.Q., Fortner, K.A., Budd, R.C. 2008. Activation of gamma delta T cells by *Borrelia burgdorferi* is indirect via a TLR- and caspase-dependent pathway. *J Immunol*, 181: 2392-8.

38. Fang, H., Welte, T., Zheng, X., Chang, G.J., Holbrook, M.R., Soong, L., Wang, T. 2010. gammadelta T cells promote the maturation of dendritic cells during West Nile virus infection. *FEMS Immunol Med Microbiol*, 59: 71-80.
39. Xu, S., Han, Y., Xu, X., Bao, Y., Zhang, M., Cao, X. 2010. IL-17A-producing gammadeltaT cells promote CTL responses against *Listeria monocytogenes* infection by enhancing dendritic cell cross-presentation. *J Immunol*, 185: 5879-87.
40. Price, S.J., Hope, J.C. 2009. Enhanced secretion of interferon-gamma by bovine gammadelta T cells induced by coculture with *Mycobacterium bovis*-infected dendritic cells: evidence for reciprocal activating signals. *Immunology*, 126: 201-8.
41. Xu, R., Wang, R., Han, G., Wang, J., Chen, G., Wang, L., Li, X., Guo, R., Shen, B., Li, Y. 2010. Complement C5a regulates IL-17 by affecting the crosstalk between DC and gammadelta T cells in CLP-induced sepsis. *Eur J Immunol*, 40: 1079-88.
42. Niedbala, W., Cai, B., Wei, X., Patakas, A., Leung, B.P., McInnes, I.B., Liew, F.Y. 2008. Interleukin 27 attenuates collagen-induced arthritis. *Ann Rheum Dis*, 67: 1474-9.
43. Pickens, S.R., Chamberlain, N.D., Volin, M.V., Mandelin, A.M., 2nd, Agrawal, H., Matsui, M., Yoshimoto, T., Shahrara, S. 2011. Local expression of IL-27 ameliorates collagen induced arthritis. *Arthritis Rheum*.
44. Naor, D., Nedvetzki, S., Walmsley, M., Yayon, A., Turley, E.A., Golan, I., Caspi, D., Sebban, L.E., Zick, Y., Garin, T. *et al.* 2007. CD44 involvement in autoimmune inflammations: the lesson to be learned from CD44-targeting by antibody or from knockout mice. *Ann N Y Acad Sci*, 1110: 233-47.
45. Szanto, S., Gal, I., Gonda, A., Glant, T.T., Mikecz, K. 2004. Expression of L-selectin, but not CD44, is required for early neutrophil extravasation in antigen-induced arthritis. *J Immunol*, 172: 6723-34.

46. Lubberts, E., van den Bersselaar, L., Oppers-Walgreen, B., Schwarzenberger, P., Coenen-de Roo, C.J., Kolls, J.K., Joosten, L.A., van den Berg, W.B. 2003. IL-17 promotes bone erosion in murine collagen-induced arthritis through loss of the receptor activator of NF-kappa B ligand/osteoprotegerin balance. *J Immunol*, 170: 2655-62.
47. Kelchtermans, H., Schurgers, E., Geboes, L., Mitera, T., Van Damme, J., Van Snick, J., Uyttenhove, C., Matthys, P. 2009. Effector mechanisms of interleukin-17 in collagen-induced arthritis in the absence of interferon-gamma and counteraction by interferon-gamma. *Arthritis Res Ther*, 11: R122.
48. Martin, B., Hirota, K., Cua, D.J., Stockinger, B., Veldhoen, M. 2009. Interleukin-17-producing gammadelta T cells selectively expand in response to pathogen products and environmental signals. *Immunity*, 31: 321-30.

FIGURE LEGENDS**Figure 1. ES-62 protects against CIA.**

(A) Clinical scores (PBS, n=43; ES-62, n=32; left-hand panel) and paw width (n=9; middle panel), expressed as mean scores \pm SEM for PBS (filled squares) or ES-62 (open squares)-treatment groups of CIA mice and disease incidence (right-hand panel), indicated by the % of animals in the PBS- (solid line) and ES-62- (broken line) groups developing a severity score ≥ 1 . (B) Serum IL-17 levels are plotted, as the means of triplicate analyses from individual mice showing a significant correlation with clinical score (number of XY pairs = 26, Pearson $r = 0.6050$; $p < 0.001$; left-hand panel) and as mean values of triplicate IL-17 analyses of serum from individual mice (naïve, n = 16; PBS, n = 26; ES-62, n = 23; right-hand panel). (C) The % IL-17⁺ DLN cells after *ex vivo* stimulation with PMA plus ionomycin; (PBS, n=19, ES-62, n=15; left-hand panel) and the % IL-17⁺ joint cells (PBS, n=11, ES-62, n=8; right-hand panel). (D) Mean values \pm SEM of ROR γ t/GAPDH mRNA (PBS, n = 4, ES-62, n = 3) as plotted for individual mice.

Figure 2. ES-62 targets IL-17-producing CD4⁺ and $\gamma\delta$ T cells.

(A) Exemplar plots of gating strategy of intracellular IL-17 expression by DLN cells from PBS- and ES-62-treated mice with CIA show forward scatter (FSC) on the x-axis versus IL-17 expression on the y-axis as well as the cellular expression of IL-17 by CD4 and $\gamma\delta$ T cells. (B) The numbers of CD4⁺ T cells (left-hand panel) and $\gamma\delta$ T cells (right hand panel) present in the DLN of individual mice (naïve, n=12; PBS, n= 19 and ES-62, n= 15) are shown. (C) Percentages of IL-17⁺ CD4⁺ T cells (naïve, n=12; PBS, n=19; ES-62, n=15; left hand panel;) after PMA plus ionomycin and IL-17⁺ $\gamma\delta$ T cells (naïve, n=8; PBS, n=11; ES-62, n=9; right hand panel) spontaneously producing IL-17 cells in the DLN of individual mice. (D) Absolute numbers of IL-17⁺ CD4⁺ T cells (naïve, n=12; PBS, n=19; ES-62, n=15; left hand

panel;) after PMA plus ionomycin exposure and IL-17⁺ $\gamma\delta$ T cells (naïve, n=8; PBS, n=11; ES-62, n=9; right hand panel) spontaneously producing IL-17 cells in the DLN of individual mice.

Figure 3: ES-62 down-regulates DC driven Th17 cell priming *in vitro*.

bmDCs from naïve (A) or CIA (B) DBA/1 mice were preincubated \pm ES-62 for 24h prior to stimulation \pm LPS (24h) before analysis of TNF- α , IL-6 and IL-23. Data are means (of mean values of triplicate samples) \pm SEM from individual mice (A; RPMI, n=5; ES-62, n=4; B; RPMI, n=7; ES-62, n=4). (C) Spontaneous production of IL-6 from bmDCs from naïve, CIA (PBS) or ES-62-treated CIA (ES-62) DBA/1 mice is presented as means (of mean values of triplicate samples) \pm SEM, n=4 individual mice. (D) OVA-pulsed LPS-matured or immature (RPMI) C57BL/6 bmDCs, preincubated \pm ES-62, were co-cultured with naïve OTII T cells for 4 d before measuring IL-17 levels by ELISA. Data are mean values \pm SD of triplicate samples from a single experiment (left-hand panel) or pooled results from 5 independent experiments where data were normalized to the LPS response at 300 nM OVA and presented as mean % maximum (LPS) response \pm SEM (right-hand panel).

Figure 4: ES-62 directly inhibits Th17 polarisation *in vitro*.

(A) Th17 cells were differentiated *in vitro* \pm ES-62 (0-1 μ g/mL) and IL-17 measured. ELISA data are presented as mean values \pm SD of triplicate samples from a single representative experiment (left-hand panel) or pooled from three independent experiments where the levels of IL-17 were normalized relative to the control Th17 cells (100%=no ES-62) and presented as the mean value \pm SEM (middle panel). IL-17 mRNA expression levels relative to GAPDH are presented where the data represent the mean values \pm SD of triplicate samples from a single experiment (right-hand panel). (B) Expression of ROR γ t, surface TLR4 and MyD88

during *in vitro* Th17 polarisation was evaluated by flow cytometric analysis. Expression levels are shown at d-0 (tinted grey trace), d-2 (thin black line) and d-4 (thick black line) relative to isotype controls (broken line). (C) Expression of MyD88 (black line) was reduced by ES-62 (1 $\mu\text{g/ml}$; grey line) as indicated by flow cytometric analysis (left-hand panel) and geometric mean analysis (MFI; right-hand panel) and (D) MyD88 mRNA expression relative to GAPDH is presented where data represent the mean values \pm range from two independent experiments.

Figure 5: ES-62 modulates crosstalk between $\gamma\delta$ T cells and DCs *in vitro*.

(A) $\gamma\delta$ T cells from BALB/c mice were activated *in vitro* with rIL-1+rIL-23 \pm ES-62 (2 $\mu\text{g/mL}$) and IL-17 release (means \pm SD n=3; left-hand panel) and CD44 expression (resting, grey; rIL-1+rIL-23, line; rIL-1+rIL-23+ES-62, bold line; right-hand panel) analysed at 24 h.

(B) The % of $\gamma\delta$ T cells expressing CD44 in DLN from PBS- and ES-62-treated CIA mice.

(C) Resting, activated (act) or ES-62-exposed activated (ES act) $\gamma\delta$ T cells and LPS-activated DCs were co-cultured at the indicated cell ratios and IL-17 detected at 24 h. Data are mean values \pm SD, n=3 from a single experiment or pooled normalized (% activated $\gamma\delta$ T cell control response) presented for each ratio as mean (of mean values) \pm SEM, n=4 independent experiments. IL-17 and ROR γ t mRNA levels relative to GAPDH were measured; data represent mean \pm SD, n=3 from a single representative experiment. (D) LSC analysis of B220⁺ (black) cells and % of $\gamma\delta$ TCR⁺ cells (grey) within B cell follicles, gated as described in Methods. Plotted data are mean % (of two sections) \pm SEM n=8 individual mice for both PBS and ES-62-treated CIA.

Figure 6: ES-62 suppresses the levels of IL-17-producing cells in the joints of CIA mice.

(A) Joint sections of naïve, PBS (articular scores 7& 8) and ES-62 treated (articular scores 3& 0) were imaged (magnification x20) for IL-17 (red) and nuclei (blue). Isotype control

sections were IL-17 negative. Synovium (Sy), Pannus (P), Articular Cavity (Ac) and Bone (B) regions are indicated. IL-17⁺ cells in the bone (B) and synovium (C) derived from panel A are from the annotated (1-4) regions of PBS sections (magnification x40). A multinucleated cell (B) is indicated by the white arrow and yellow bars indicate relative magnification (C; left-hand panel 20 μm scan zoom 2.3, right-hand panel 10 μm scan zoom 2.1; D; left-hand panel 5 μm scan zoom 2.5, right-hand panel 20 μm scan zoom 2.6). A model of the mechanism of action of ES-62 (D) modulating a complex network of DC-CD4⁺T cell and γδ T cell interactions to suppress pathogenic IL-17 responses in CIA is shown.

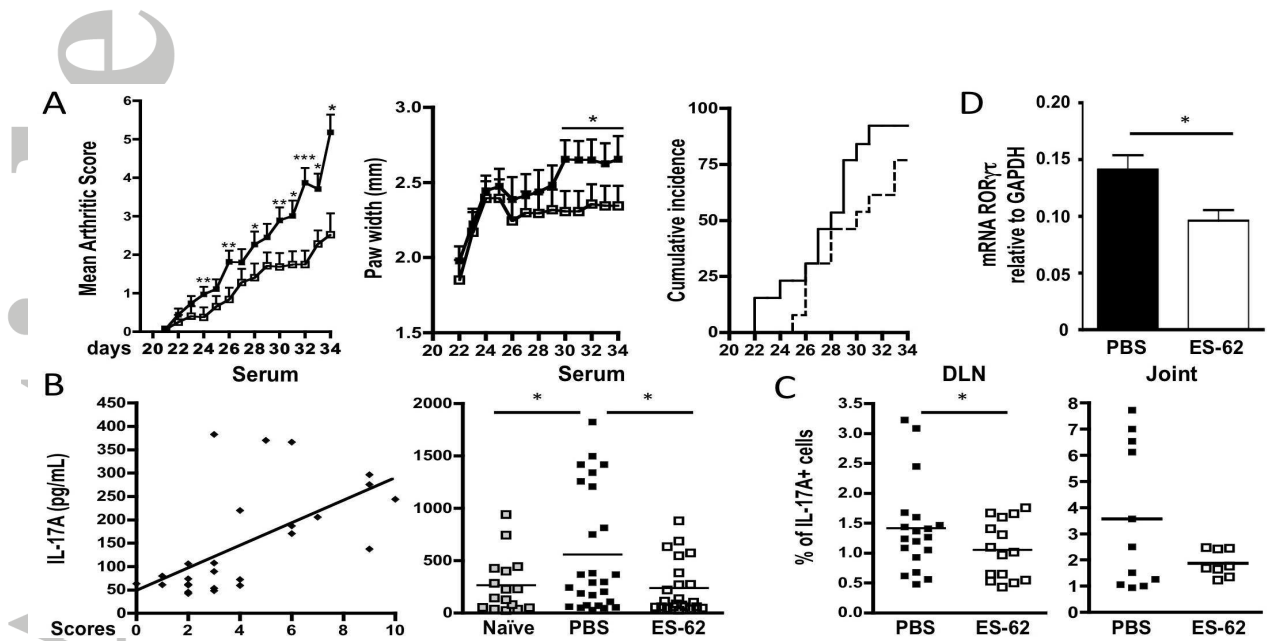
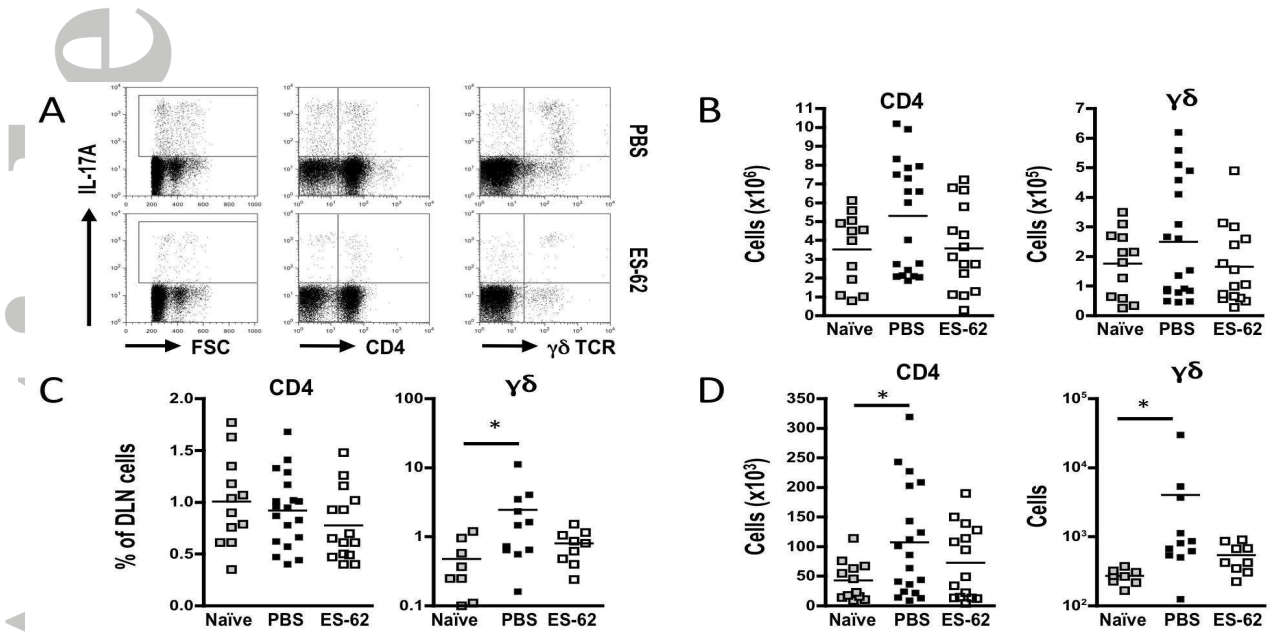


Figure 1. ES-62 protects against CIA. (A) Clinical scores (PBS, n=43; ES-62, n=32; left-hand panel) and paw width (n=9; middle panel), expressed as mean scores \pm SEM for PBS (filled squares) or ES-62 (open squares)-treatment groups of CIA mice and disease incidence (right-hand panel), indicated by the % of animals in the PBS- (solid line) and ES-62- (broken line) groups developing a severity score \geq 1. (B) Serum IL-17 levels are plotted, as the means of triplicate analyses from individual mice showing a significant correlation with clinical score (number of XY pairs=26, Pearson $r=0.6050$; $p<0.001$; left-hand panel) and as mean values of triplicate IL-17 analyses of serum from individual mice (naïve, n=16; PBS, n=26; ES-62, n=23; right-hand panel). (C) The % IL-17⁺ DLN cells after *ex vivo* stimulation with PMA plus ionomycin (PBS, n=19, ES-62, n=15; left-hand panel) and the % IL-17⁺ joint cells (PBS, n=11, ES-62, n=8; right-hand panel). (D) Mean values \pm SEM of RORγt/GAPDH mRNA (PBS, n=4, ES-62, n=3) as plotted for individual mice.



Accepted

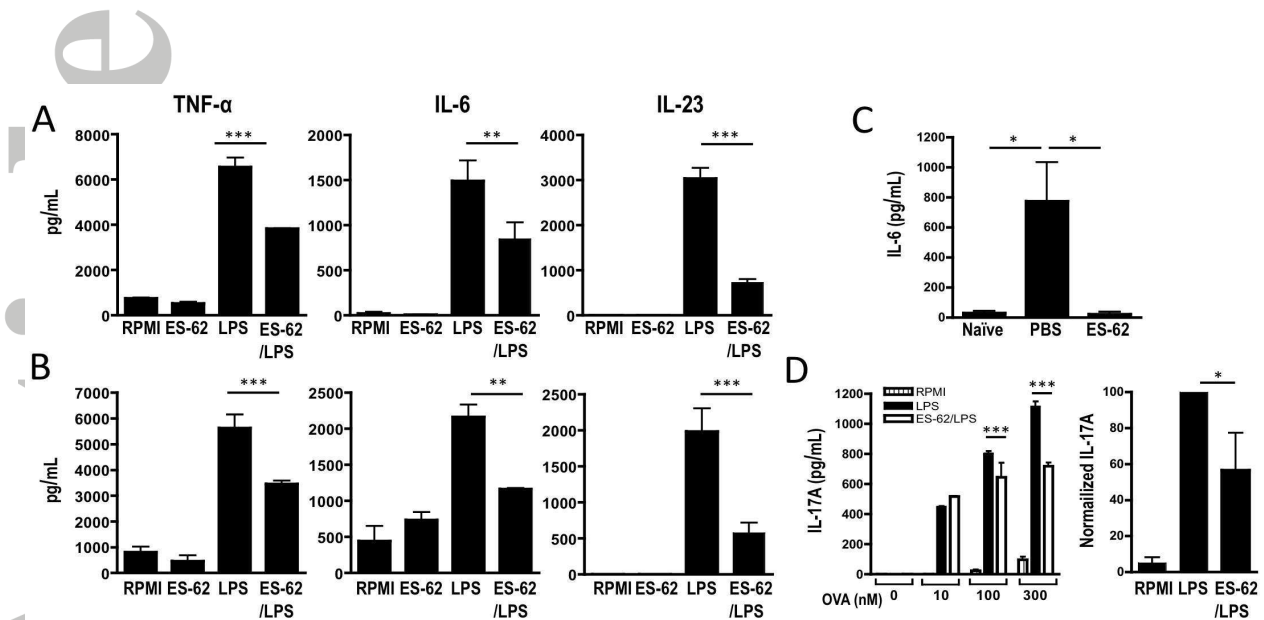


Figure 3. ES-62 down-regulates DC driven Th17 cell priming *in vitro*. bmDCs from naïve (A) or CIA (B) DBA/1 mice were preincubated ± ES-62 for 24 h prior to stimulation ± LPS (24h) before analysis of TNF- α , IL-6 and IL-23. Data are means (of mean values of triplicate samples) ± SEM from individual mice (A: RPMI, n=5; ES-62, n=4; B: RPMI, n=7; ES-62, n=4). (C) Spontaneous production of IL-6 from bmDCs from naïve, CIA (PBS) or ES-62-treated CIA (ES-62) DBA/1 mice is presented as means (of mean values of triplicate samples) ± SEM, n=4 individual mice. (D) OVA-pulsed LPS-matured or immature (RPMI) C57BL/6 bmDCs, preincubated ± ES-62, were co-cultured with naïve OTII T cells for 4 d before measuring IL-17 levels by ELISA. Data are mean values ± SD of triplicate samples from a single experiment (left-hand panel) or pooled results from 5 independent experiments where data were normalized to the LPS response at 300 nM OVA and presented as mean % maximum (LPS) response ± SEM (right-hand panel).

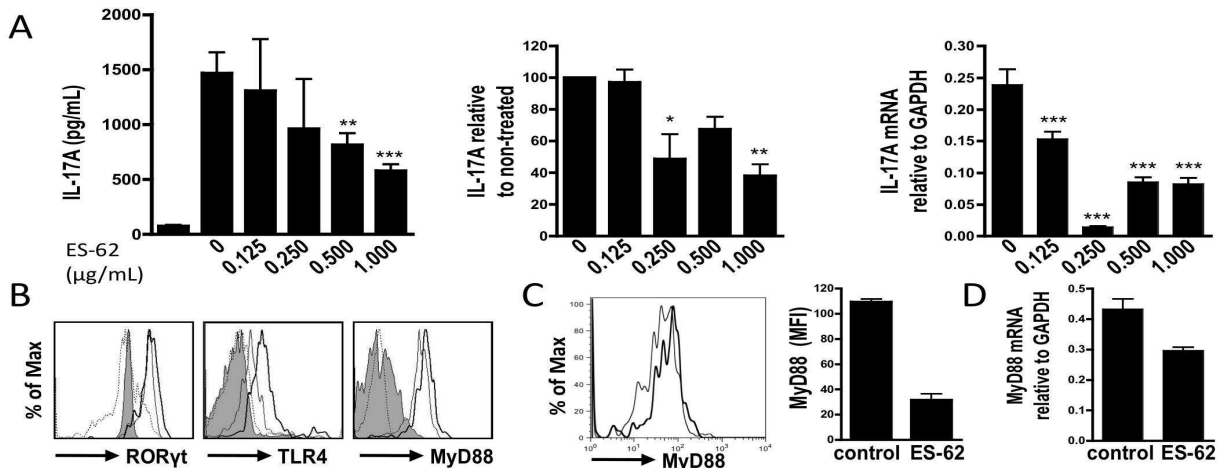


Figure 4. ES-62 directly inhibits Th17 polarisation *in vitro*. (A) Th17 cells were differentiated *in vitro* ± ES-62 (0-1 μg/mL) and IL-17 measured. ELISA data are presented as mean values ± SD of triplicate samples from a single representative experiment (left-hand panel) or pooled from three independent experiments where the levels of IL-17 were normalized relative to the control Th17 cells (100%=no ES-62) and presented as the mean value ± SEM (middle panel). IL-17 mRNA expression levels relative to GAPDH are presented where the data represent the mean values ± SD of triplicate samples from a single experiment (right-hand panel). (B) Expression of RORγt, surface TLR4 and MyD88 during *in vitro* Th17 polarisation was evaluated by flow cytometric analysis. Expression levels are shown at d-0 (tinted grey trace), d-2 (thin black line) and d-4 (thick black line) relative to isotype controls (broken line). (C) Expression of MyD88 (black line) was reduced by ES-62 (1 μg/ml; grey line) as indicated by flow cytometric analysis (left-hand panel) and geometric mean analysis (MFI; right-hand panel) and (D) MyD88 mRNA expression relative to GAPDH is presented where data represent the mean values ± range from two independent experiments.

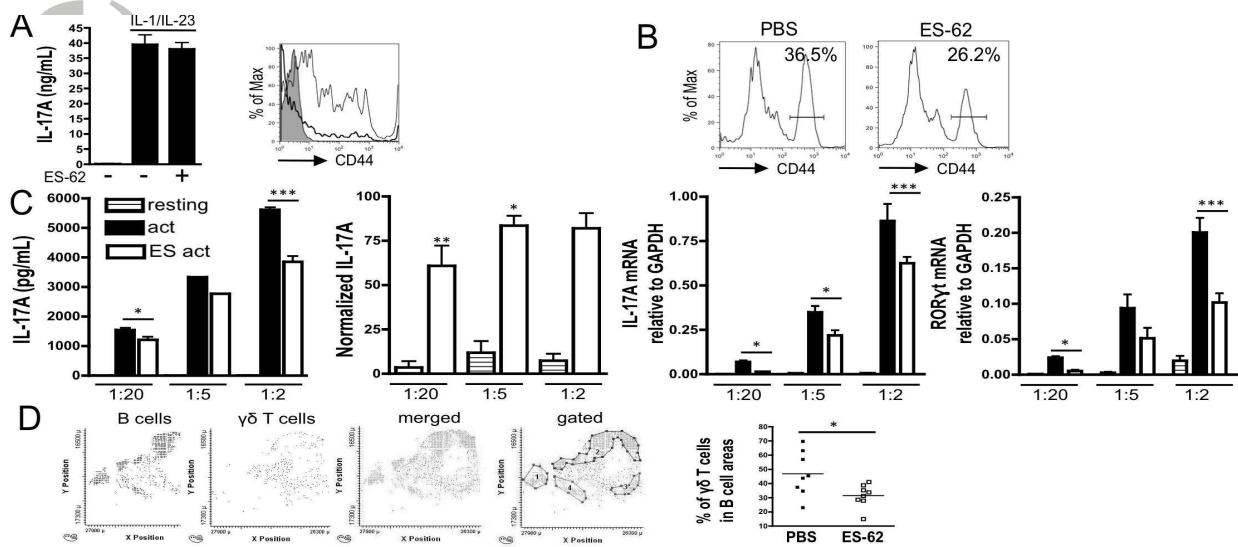


Figure 5. ES-62 modulates crosstalk between $\gamma\delta$ T cells and DCs *in vitro*. (A) $\gamma\delta$ T cells from BALB/c mice were activated *in vitro* with rIL-1+rIL-23 \pm ES-62 (2 μ g/mL) and IL-17 release (means \pm SD n=3; left-hand panel) and CD44 expression (resting, grey; rIL-1+rIL-23, line; rIL-1+rIL-23+ES-62, bold line; right-hand panel) analysed at 24 h. (B) The % of $\gamma\delta$ T cells expressing CD44 in DLN from PBS- and ES-62-treated CIA mice. (C) Resting, activated (act) or ES-62-exposed activated (ES act) $\gamma\delta$ T cells and LPS-activated DCs were co-cultured at the indicated cell ratios and IL-17 detected at 24 h. Data are mean values \pm SD, n=3 from a single experiment or pooled normalized (% activated $\gamma\delta$ T cell control response) presented for each ratio as mean (of mean values) \pm SEM, n=4 independent experiments. IL-17 and ROR γ t mRNA levels relative to GAPDH were measured; data represent mean \pm SD, n=3 from a single representative experiment. (D) LSC analysis of B220⁺ (black) cells and % of $\gamma\delta$ TCR⁺ cells (grey) within B cell follicles, gated as described in Methods. Plotted data are mean % (of two sections) \pm SEM n=8 individual mice for both PBS and ES-62-treated CIA.

Accepted

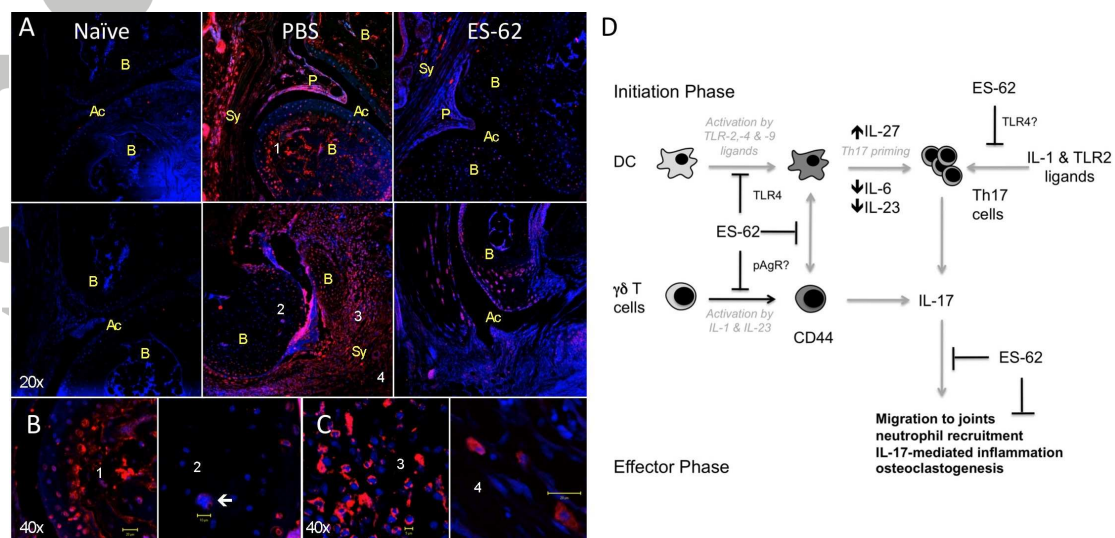


Figure 6. ES-62 suppresses the levels of IL-17-producing cells in the joints of CIA mice. (A) Joint sections of naïve, PBS (articular scores 7&8) and ES-62 treated (articular scores 3&0) were imaged (magnification x20) for IL-17 (red) and nuclei (blue). Isotype control sections were IL-17 negative. Synovium (Sy), Pannus (P), Articular Cavity (Ac) and Bone (B) regions are indicated. IL-17⁺ cells in the bone (B) and synovium (C) derived from panel A are from the annotated (1-4) regions of PBS sections (magnification x40). A multinucleated cell (B) is indicated by the white arrow and yellow bars indicate relative magnification (C; left-hand panel 20 μm scan zoom 2.3, right-hand panel 10 μm scan zoom 2.1; D; left-hand panel 5 μm scan zoom 2.5, right-hand panel 20 μm scan zoom 2.6). A model of the mechanism of action of ES-62 (D) modulating a complex network of DC-CD4⁺T cell and γδ T cell interactions to suppress pathogenic IL-17 responses in CIA is shown.